

## CHAPTER V

### FILAMENTATION IN HEAVY ION COLLISIONS

In this chapter filamentation instability of two counter streaming color fluxes will be analyzed. This chapter is composed as follows. In section 5.1 motivation for studying the filamentation will be provided. In section 5.2 the derivation of the equations describing filamentation of two color streams will be presented. Section 5.3 deals with the numerical solutions and their analysis. Summary and conclusions are provided in section 5.4.

**5.1 INTRODUCTION :** The prospects of generating QGP in the relativistic heavy-ion collision (RHIC) experiments have stimulated much interest in finding out the consequence of the presence of QGP on the evolution of secondaries. Such studies may be useful in explaining the new features of RHIC which would possibly arise due to the presence of QGP and also in finding out the signature of QGP. Due to the expected transparency of the nuclei in RHIC, the instabilities associated with the plasma streaming are of interest. Such instabilities associated with the hadron plasma were first studied by Ivanov<sup>1</sup> and it was demonstrated that under RHIC conditions only the filamentation mode is the most unstable as the growth time of this instability was found to be shorter than that of the total interaction time of the two nuclei [i.e. the time interval within which the two nuclei can fly pass each other's diameters, see Ivanov in ref.1]. Soon after this work it was shown that filamentation instability in RHIC might occur even at the energy range ( few hundred GeV per nucleon)

where quark-gluon plasma might be produced.<sup>2</sup> Dispersion relation and the growth rate for the filamentation mode, in these works, have been obtained within the frame work of classical kinetic theory.

Thus, it is obviously of interest to examine how the filamentation instability can affect heavy ion collisions. Filamentation is the instability which leads to stratification of initially homogeneous and oppositely directed plasma flux<sup>3</sup> which are interacting via mean vector fields (gluon fields for QGP). As filamentation instability leads to net color and baryon current in the plasma it was proposed in the previous work in hadron plasma and in QGP (see Ref. 1-2) that such stratification can directly be observed in the heavy ion collision experiments. This is because such currents should be radiating electromagnetic waves ( $\gamma$  radiation) along the direction perpendicular to the beam axis [Ref.1-2]. However, doubts have been cast on this way of detecting the instability<sup>4</sup> on the ground that there are other photon sources, e.g. neutral pions, which can also emit photons in the same energy range as those from filamentation

Another important consequence of the instability is that it might enhance the nuclear stopping power. As we will see below (in section 5.2) in such an instability, the electric field is directed against the streaming current. This can decelerate the streaming velocity. However, this mechanism can become strong only when the electric field grows in amplitude with the instability. This is a collective mechanism for the deceleration and it becomes important only after the growth time of the instability. Thus, to examine such a deceleration, the study of the nonlinear state generated by the

instability is of much importance. If the growth time of the instability is much shorter than the overall interaction time of the two nuclei then the deceleration can become significant and may enhance the stopping power of the nuclei. Indeed, there are some indications that stopping power of nucleus-nucleus collision is higher than that of nucleon-nucleon or nucleon-nucleus collisions at high energies<sup>5</sup>. It ought to be mentioned that in the earlier works on the filamentation in QGP (Ref.2-3) the problem of stopping has not been analyzed. However, in the work on filamentation in the hadron plasma (Ref.1) it was mentioned that such instability might contribute to nuclear stopping.

In the present work our chief interest is to examine how effective is the collective deceleration mechanism provided by the filamentation. As already mentioned, this can affect the nuclear stopping. For this the analysis of the nonlinear state generated by the instability will be of crucial importance. We have applied the CHD equations, derived in the previous chapter, to study this instability non-perturbatively. However, in the present section a linear stability analysis will also be provided to obtain the dispersion relation for the filamentation mode. The maximum growth rate obtained by using the CHD equations is found to be the same as that obtained by using the linearized kinetic equations.<sup>4</sup>

For simplicity we have considered the plasma to be infinite in extent and comprising of two counter streaming color beams in the color neutralizing background. Moreover, we have considered the simplest geometry in which filamentation can occur. This is consistent with the earlier work as they have demonstrated that the filamentation

mode is the most unstable mode, for RHIC conditions, compared to other possible instabilities arising due to the plasma streaming (Ref.1-3). Thus we have considered a mixed wave (having both longitudinal and transverse components of the color fields) having a component of the color electric field in the direction of the stream velocity and thus generating a current in the opposite direction. The propagation of waves along the beam direction is ignored as it gives the "longitudinal two stream instability"<sup>3</sup> which is found to be much weaker, in RHIC conditions, as compared to the filamentation mode.<sup>4</sup>

In order to analyze the stopping of the beams and to describe the properties of the final nonlinear state of the instability, we have numerically investigated the solutions of the nonlinear hydrodynamics and the field equations using a plane wave ansatz. Starting from the arbitrary initial conditions in a moving frame (in which the wave phase is assumed to be stationary), velocity profiles in x and z-directions are studied. It is found that the non-linear state is one where the incident color fluxes have lost a considerable fraction of their mean directed motion. The auto-correlations of the velocity profiles suggest that the stream velocities have become chaotic and the mean value is never restored the original value of the directed velocity.

It should be noted that analogous to the situation in Coulomb plasma a colored test particle traversing in QCD plasma can lose its energy by interactions with plasma collective modes. Indeed, the perturbative calculations of such type, for equilibrium QGP, have shown that the energy loss of a high energy test particle is extremely small<sup>6</sup>

**5.2 EQUATIONS FOR FILAMENTATION :** To obtain the basic equations describing the filamentation we apply the CHD and Yang-Mills equations, in cold collisionless limit, to the following situation :We assume that two species  $A = 1,2$  of the same masses are counter streaming in  $z$ -direction. The equilibrium velocities  $V_{Ao}^z$ , when no perturbation is applied, for both the species is  $V_o$  for  $A = 1$  and  $-V_o$  for  $A = 2$  and  $|V_o| \sim 1$ . The equilibrium components of velocity vector in the other direction (perpendicular to  $z$ ) are assumed to be zero. When there is no perturbation, both the species are considered to be homogeneous and have the same value for the equilibrium density  $n_o$ . Also the color vectors of both species are assumed to be the same in the absence of any perturbation i.e  $I_{1oa} = I_{2oa}$ . There is an overall color neutralizing back ground which is homogeneous in density and color and does not change with the perturbations. It was found that the instability is maximum in the direction perpendicular to the stream velocity<sup>1</sup>. Therefore in such a plasma we have considered a mixed wave which propagates in a direction perpendicular (say  $x$ -axis) to the stream axis. The wave is assumed to have components of color electric fields along  $x$ - and  $z$ -axes while the component of color magnetic field is in  $y$ -direction. Such a system is unstable and leads to filamentation (Ref.1-4). The CHD and Yang-Mills equations for this case are then written as

$$\begin{aligned}
 (\partial_0^2 - \partial_x^2)A_a^z + g\epsilon_{abc}[2A_b^x \partial_x A_c^z + \partial_x A_b^x A_c^z] + g^2[(A_b^x)^2 A_a^z - (A_b^x A_b^z A_a^x)] \\
 = J_a^z \quad (1)
 \end{aligned}$$

$$\partial_0^2 A_a^x - g\epsilon_{abc} A_b^x \partial_x A_c^x + g^2 [(A_b^z)^2 A_a^x - (A_b^x A_b^z) A_a^z] = J_a^x \quad (2)$$

$$\partial_0 n_A + \partial_x (n_A V_A^x) = 0 \quad (3)$$

$$m(\partial_0 + V_A^x \partial_x) V_A^x = g I_{Aa} [E_a^x - V_A^z B_a^y - V_A^x (V_A^x E_a^x + V_A^z E_a^z)] S_{QA} \quad (5)$$

$$m(\partial_0 + V_A^x \partial_x) V_A^z = g I_{Aa} [E_a^z - V_A^x B_a^y - V_A^z (V_A^x E_a^x + V_A^z E_a^z)] S_{QA} \quad (6)$$

$$(\partial_0 + V_A^x \partial_x) I_{Aa} = g\epsilon_{abc} (V_A^x A_b^x + V_A^z A_b^z) I_{Ac} \quad (7)$$

where  $S_{QA} = \{1 - (V_A^x)^2 - (V_A^z)^2\}^{1/2}$ ,  $E_a^x = -\partial_0 A_a^x$ ,  $E_a^z = -\partial_0 A_a^z$  and  $B_a^y = -\partial_x A_a^z + g\epsilon_{abc} A_b^x A_c^z$ . It should be mentioned that  $A_0 = 0$  is the gauge choice exercised in writing the above equations.

Before we proceed further, it should be noted that interpenetration of the two species can cause collisional momentum transfer from one specie to another. Therefore in Eqs.(4-5) one must include a term involving collisions between particles belonging to the two different species. Such terms may be included phenomenologically as in the appendix of Chapter IV. However, when the plasma frequency is much higher than the collision frequency, such terms in the momentum balance equations (i.e. Eqs.4-5) can be ignored. This is because the momentum transfer due to the collective mechanism can significantly exceed that due to the collisions.

Next we obtain the dispersion relation for the instability. For this purpose we will assume that when no perturbation is applied, all the force field in the plasma is zero. Such a plasma will be then shown to be unstable with respect to the transverse perturbations

provided by the mixed wave. Since for the stability analysis we are interested in small departure from the equilibrium, we write

(i)  $A_a^z = \tilde{A}_a^z$ ,  $A_a^x = \tilde{A}_a^x$  as there is no background Yang-Mills potentials

(ii) no initial flow in the x-direction i.e.  $V_a^x = \tilde{V}_a^x$

(iii)  $V_A^z = V_{A0} + \tilde{V}_A^z$  ( $V_{A0} = -V_0$  for  $A = 1$  and  $+V_0$  for  $A = 2$ )

(iv) as the background color vectors are same we write  $I_{Aa} = I_a^0 + \tilde{I}_{Aa}$  and

(v) also the background density for both the species are the same and hence  $n_A = n_0 + \tilde{n}_A$ .

Here all the quantities with 'tilde' denote perturbations. The absolute values of the background quantities are assumed to be much greater than the absolute values of the perturbations. Moreover all the background quantities are assumed to be homogeneous in space and constant in time. The various quantities are substituted in eqs. (1)-(6) and by retaining only the I order terms in the perturbations, one can get the 'linearized' version of Eqs.(1)-(6).

Next by considering that all the perturbed quantities vary as  $\sim e^{i(kx-\omega t)}$ , one can obtain from the CHD eqs:

$$\tilde{n}_A = -(k/\omega)n_0 g SQ_0 I_b^0 (\omega \tilde{A}_b^x + k V_{A0}^z \tilde{A}_b^z) / (m \omega)$$

$$\tilde{V}_A^x = -g I_b^0 (\omega \tilde{A}_b^x + k V_{A0}^z \tilde{A}_b^z) / (m \omega)$$

$$\tilde{V}_A^z = -g SQ_0 I_b^0 \tilde{A}_b^z / (m \omega)$$

where  $SQ_0 = \left\{ 1 - V_0^2 \right\}^{1/2}$ .

If we substitute these in the expression for the currents (Chapter II) we get the following current profile

$$\tilde{J}_a^z = - \frac{2 g^2 \rho_0}{m} I_{ab}^0 \tilde{\chi}_b^z + \frac{2 i g^2 n_0}{\omega} V_0^2 \epsilon_{abc} \tilde{A}_b^z I_c^0 - 2(k/\omega) \frac{g^2 \rho_0}{m} V_0^2 I_{ab}^0 \tilde{\chi}_b^z \quad (7)$$

where  $\rho_0 = n_0 \cdot [1 - V_0^2]^{1/2}$  is the density in the rest frame of the fluid ( i.e. proper density ).

As a result the linearized en. (6) then reduces to  $-(\omega^2 - k^2) \tilde{A}_a^z = \tilde{J}_a^z$

Multiplying these eqs by  $I_a^0$  and summing over a, we get,

$$-(\omega^2 - k^2) = -2\omega_p^2 (1 - V_0^2) - 2(k/\omega)\omega_p^2 V_0^2 \quad (8)$$

where  $\omega_p^2 = \frac{g \rho_0 (I_a^0)}{m}$ .

The solutions of eq. (8) are,

$$\omega_{\pm}^2 = \frac{\left[ k^2 + 2\omega_p^2(1-V_0^2) \right] \pm \left[ \left\{ k^2 + 2\omega_p^2(1-V_0^2) \right\}^2 + 8k^2\omega_p^2 V_0^2 \right]^{1/2}}{2} \quad (9)$$

Clearly the -ve root of this equation gives rise to an instability For the streams colliding with the relativistic velocity  $V_0 \sim 1$ , eq. (9) will become

$$\omega_-^2 = \frac{k^2}{2} \left[ 1 - \left\{ 1 + 8\omega_p^2/k^2 \right\}^{1/2} \right] \quad (10)$$

One can see from (10) that the absolute value of  $\omega_-^2$  always increases with  $k^2$  For  $k^2 \gg \omega_p^2$  one finds

$$\omega_-^2 \cong -\omega_0^2 (1 - \omega_0^2/k^2) \quad (11)$$

where  $\omega_0 = 2\omega_p$  which is similar to that obtained by Mrowczynski (Ref.4). Retaining only zeroth order term in  $\omega_0/k$  one can get the minimum time  $t_{\min}$  scale for the instability to develop as

$$t_{\min} = |\omega|^{-1} \sim \frac{0.7}{\omega_p} \sim 0.5-0.3 \text{ fm/ c}$$

This instability can grow if the interaction time of the two nuclei is greater than  $t_{\min}$ . The interaction time  $t_{\text{int}}$  of two nuclei can be taken as the time the nuclei will take to fly pass each other

$$t_{\text{int}} \sim 2 r_0 A_0 \left( 2 M_N / E_{\text{lab}} \right)^{1/2} \quad (12)$$

where  $r_0 = 1.1 \text{ fm}$ ,  $A$  is atomic number,  $E_{\text{lab}}$  is the energy of the projectile. At 200 GeV/nucleon, for the collision of two uranium nuclei  $t_{\text{int}} \sim 1.5 \text{ fm/c}$ , which is much greater than  $t_{\min}$  and hence the instability can develop in RHIC. Note that  $t_{\text{int}}$  is underestimated as the mutual deceleration of the two species due to collisions and the effect of plasmon decay are ignored (Ref.1,4). However, this underestimate is justified.

In order to estimate the strength of initial perturbations of the gauge fields  $A$ , we take  $\frac{E^2}{\epsilon_{\text{ther}}} \sim \beta \sim 10^{-1}$  where  $\beta$  is the plasma parameter (see chapter IV, page 9) and  $E^2$  is the field energy. Thus  $\frac{\omega_p^2 A^2}{\epsilon_{\text{ther}}} \sim \frac{g^4 T^4 A^2}{T^4} \sim g^4 A^2$  and thus  $A \sim 10^{-1}$ . Hence within the time period of few  $t_{\min}$  the perturbations can become large and they cannot be described by the linearized set of equations (Eqs.7-9). In order to study the nonlinear state generated by the instability one must consider the solutions of Eqs(1-6) with the full non-linearity. However Eqs.(1-6) are a set of coupled nonlinear partial differential equations, which are very difficult to solve in their generality. Therefore, we look for special solutions of these equations which are nonlinear plane stationary waves. Thus we assume that all the quantities are function of a single variable  $\zeta = x + \beta t$ . This assumption will convert all the partial differential equations of the

problem to the ordinary ones. Physically the important assumption here is that the nonlinear solutions are stationary in a frame moving with the phase speed  $\beta$ . Such stationary waves have already been discussed in Chapter III.

In the stationary frame all the hydrodynamical equations, except the one for color dynamics for (say) specie 1 can be integrated analytically. In the dimensionless form the resultant equations are given below

$$v_A^x = -\beta + \beta \left[ 1 - \left\{ \beta^2 + \frac{f_{1A}}{1 + f_A} \right\} \left\{ 1 - \frac{f_{1A}^2}{1 + f_A^2} \right\} \right]^{1/2} \quad (13)$$

$$v_A^z = \frac{\left\{ 1 - (\theta v_A^x)^2 \right\}^{1/2}}{\theta \left\{ 1 + f_A^2 \right\}} f_A \quad (14)$$

$$n_A = \frac{\beta n_o}{\beta + \theta v_A^x} \quad (15)$$

$$I_{2a} = \beta \theta k \epsilon_{abc} A_b^x A_c^{x'} + \frac{(\beta^2 - 1)}{\beta} \theta k \epsilon_{abc} A_b^z A_c^{z'} + \theta k^2 [(A_b^z)^2 A_a^x - (A_b^x A_b^z) A_a^z] - I_{1a} + 2I_{2oa} \quad (16)$$

$$\text{where } f_A = \frac{v_{Ao}^z}{\left\{ 1 - v_o^2 \right\}^{1/2}} - \theta I_{Ab} A_b^z$$

$$f_{1A} = \frac{1}{\left\{ 1 - v_o^2 \right\}^{1/2}} - \beta \theta I_{Ab} A_b^x$$

$$\theta = \frac{g_1 a_o}{m}, \quad k = \frac{g a_o}{\omega_p} \quad \text{and} \quad \omega_p^2 = \frac{g^2 i_o^2 n_o}{m}$$

Here  $a_o$  and  $i_o$  are some normalizing factors for the dimensionless

gauge field potentials and the color vector respectively and they arise in the same way as before (see previous chapters). The prime denotes differentiation with respect to a dimensionless variable  $t$  defined by  $t = \zeta/\omega_p$ . These equations then can be used to define current profiles in terms of the gauge field amplitudes. When these current profiles are substituted in the Yang-Mills equations one obtains a set of equations, in terms of the dimensionless variables, which describe the saturated nonlinear state generated by the filamentation instability in the stationary frame

$$I'_{1a} = \frac{\theta k}{\beta} N_1 \epsilon_{abc} \left[ V_1^x A_b^x + V_1^z A_b^z \right] I_{1c} \quad (17)$$

$$\beta^2 A_a^{x''} - k \epsilon_{abc} A_b^z A_c^z + k^2 \left[ (A_b^z)^2 A_a^x - (A_b^x A_b^z) A_a^z \right] = J_a^x \quad (18)$$

$$(\beta^2 - 1) A_a^{z''} + k \epsilon_{abc} \left[ 2 A_b^x A_c^z + A_b^z A_c^x \right] + k^2 \left[ (A_b^x)^2 A_a^z - (A_b^x A_b^z) A_a^x \right] = J_a^z \quad (19)$$

This is a set of 15 coupled ordinary nonlinear equations and it is not possible to solve them analytically. Therefore solutions of these equations have been obtained numerically and they are discussed in the next section

**5.3 NUMERICAL RESULTS AND DISCUSSION :** In this section numerical solutions of Eqs.(17-19) will be discussed. These equations have the following conservation law

$$\frac{\beta^2}{2} (A_a^x)^2 + \frac{\beta^2 - 1}{2} (A_a^z)^2 + k^2 \left[ (A_b^x)^2 (A_b^z)^2 - (A_b^x A_b^z)^2 \right] + \frac{1}{\theta} [1/SQ_1 + 1/SQ_2] = \text{constant} \quad (20)$$

where  $SQ_A$  ( $A = 1, 2$ ) have already defined above [below Eq.(7)]. Eq.(20) can be understood in terms of the field energy and the kinetic energy

of the plasma particles. The terms with the factors  $1/SQ_A$  are correspond to the sum of kinetic energy of each specie, while the rest of the terms correspond to the field energy. Eq.(20) has been used to check the accuracy of the numerical solutions.

Fourth order Runge-Kutta method with variable step size has been used to integrate Eqs.(17-19). The results shown in the figures (below) are the typical solutions of Eqs.(17-19). The solutions with different initial conditions and parameter choice do not show any different qualitative behavior than those depicted in these figures.

As mentioned earlier filamentation is expected to provide a mechanism for the deceleration of the color flux. Therefore, the velocity profiles defined by Eqs.(13-14) are the right physical variables to study such effect.

Fig (1a) shows the velocity of specie 2 in z-direction as function of t. It clearly shows that for the value of non-abelian parameter  $k = 0.1$ , the initial flow velocity (at  $t = 0$ )  $V_{20}^z = -9$  (in the units of  $\theta$ ) considerably reduces with increasing t and attains a mean value around -1.0 within the time scale characterized by a few plasma frequency. Thus the velocity of the color flux in the longitudinal direction reduces significantly. The transverse component of the velocity (in x-direction) which was zero initially has acquired a mean velocity around 3.9 during the course of the motion. One can calculate the loss in the kinetic energy by subtracting the initial kinetic energy from the mean energy. It is found that around 84% of the initial kinetic energy has been lost during the course of the motion.

Fig.(2a) shows the z-component of the velocity of the specie 2

for the strength of the non-abelian parameter  $k = 0.5$ . The plot clearly shows that the initial flow velocity  $V_{20}^z = -9$  attains a mean value around  $-3.0$  within the time period characterized by a few plasma frequency. Fig (2b) depicts the plot of x-component of the velocity. Initial flow velocity which was zero develops a mean velocity around the value  $2.7$ . The energy loss, in this case, is found to be  $90\%$  of the initial kinetic energy of the color flux.

Thus, from this one may conclude that within a few plasma oscillations ( $t_{\min}^{-1}$  included) the color fluxes will lose considerable fraction of their mean directed energy and hence enhance the nuclear stopping. The time within which the beams lose their energy may be higher than  $t_{\text{int}}$  (as estimated above). However, the overall interaction time due to this collective mechanism can exceed  $t_{\text{int}}$ .

The autocorrelation for the z-component of the velocity (Fig.1c-2c) shows that the flow has become chaotic and the correlations decrease very fast without any sign of its recurrence. Thus one can say that a significant fraction of the mean directed energy of the plasma stream is lost completely into randomly oscillating wave fields and kinetic energies.

The time interval within which the beams are losing energy may be of the order of sum of  $t_{\min}$  and the time within which the nonlinear state loses its initial kinetic energy. In the stationary frame ansatz this time may be regarded as the distance over which the fluid element has lost its energy. From our results an estimate of such distances may be of the orders of few fermis which is much less than that obtained by the linear calculations of the energy loss [Ref.6].

Fig.(3) shows the velocity profile for the case  $k = 0$ . In this

case Eqs (17-19) reduce to those for an abelian plasma as all the non-abelian terms drop out from the equations. This figure clearly shows that there is a marginal difference between the mean velocity and the initial velocity. Thus, in this case, the fluxes do not lose much of their kinetic energy compared to the previous two cases with  $k \neq 0$ .

**5.4 SUMMARY AND CONCLUSIONS :** In this chapter we have studied the filamentation instability and have found that the hydrodynamic treatment that has been adopted by us gives the same value of the maximum growth rate as obtained by the earlier methods based on classical kinetic approach.

The analysis of the nonlinear state of the instability is carried out. The nonlinear terms seem to lead to a situation where the beams have lost their directed velocity significantly for the cases  $k \neq 0$ . The estimates of the energy loss and the relaxation time indicate that, this deceleration mechanism may significantly enhance the nuclear stopping power in heavy ion collision experiments.

## REFERENCES

1. Yu.Ivanov : Nucl.Phys.A 474 693 (1987) and see also  
Yu.B. Ivanov : "The Nuclear Equation of State Part.B"  
edited by W.Griener and H.Stocker, NATO ASI series  
(Plenum Press, New York, 1989).
2. Yu.Pokrovsky and A.Selikhov : JETP Lett. 47 12 (1988).
3. R.C.Davidson : Foundation Of plasma Physics VOL. I.  
edited by A.Galeev and R.Sudan (North-Holland,  
Amsterdam,1983).
4. S.Mrowczynski : Phys.Lett.B 214 (1988).
5. W.Busza and A.Goldhaber : Phys.Lett.B 139 235 (1984)  
H.Schimdt and H.Gutbrod : "The Nuclear Equation of State"  
Part.B edited by W.Griener and H.Stocker, NATO ASI  
series (Plenum Press, New York, 1989).  
A.Marzari-Chiesa : Nucl.Phys.A 519 435c (1990).
6. M.Thoma and M.Gyulassy : Nucl.Phys.B 351 491 (1991)  
S.Mrowczynski : Phys.Lett.B 269 383 (1991).

## FIGURE CAPTION

Fig 1a z-component of the velocity of specie 2 is plotted as function of t. The values of parameters are  $\beta = 1.1$ ,  $\theta = 0.1$ ,  $V_0 = 9$  (in the units of  $\theta$ ), and  $k = 0.1$ . The initial conditions are  $I_{11} = I_{12} = I_{13} = 1$ ,  $A_a^x = A_a^z = 0$  ( $a= 1,2,3$ ) and  $A_1^{x'} = 1.4$ ,  $A_2^{x'} = 0.2$ ,  $A_3^{x'} = 0.3$ ,  $A_1^{z'} = 0.2$ ,  $A_2^{z'} = -0.3$ ,  $A_3^{z'} = 1.1$ .

Fig.1b x-component of specie 2 is plotted as function of t. All the conditions are the same as Fig.1a.

Fig 1c Autocorrelation of z-component of the velocity in Fig.1a.

Fig 2a z-component of the flow velocity of specie 2 as function of t is plotted. All the conditions are the same as Fig.1a except k which has value  $k = 0.5$ .

Fig.2b x-component of the velocity is plotted as function of t and all the conditions are the same as those in Fig.2a.

Fig.2c Autocorrelation of z-component of velocity in Fig.2a.

Fig.3 x-component of velocity of specie 2 is plotted as function for  $k = 0$  (abelian case) and all other conditions are same as Fig.1a.

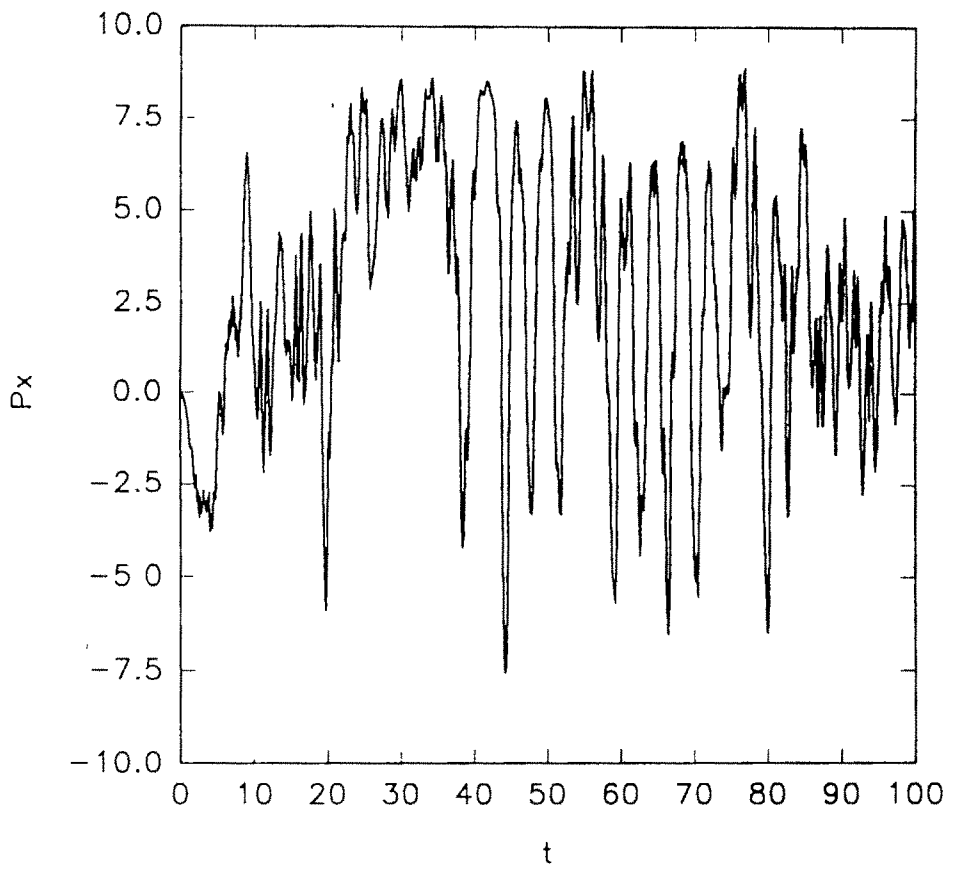


Fig 1b

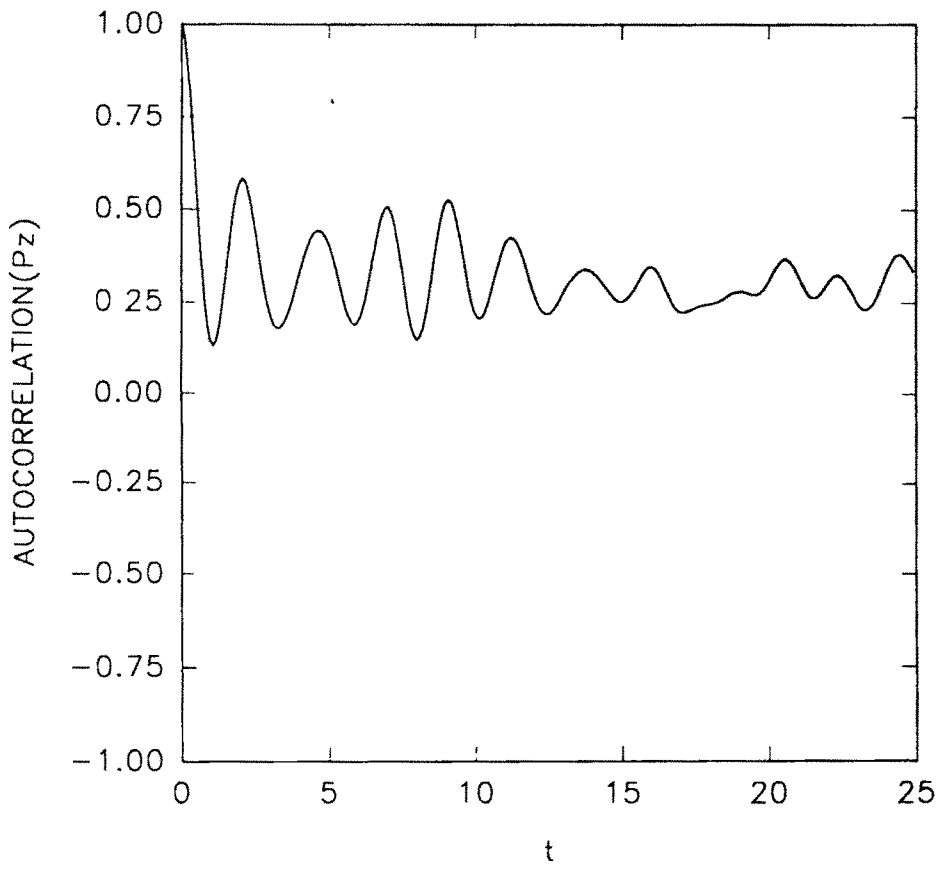


Fig 1c

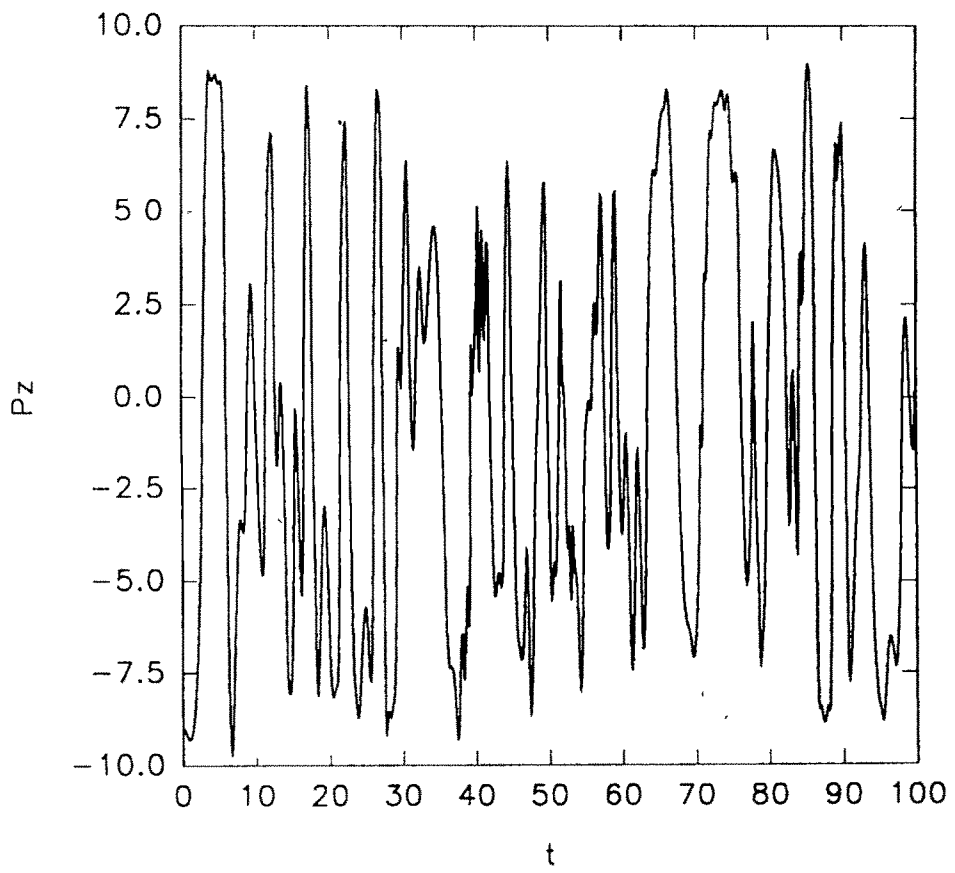


Fig 2a

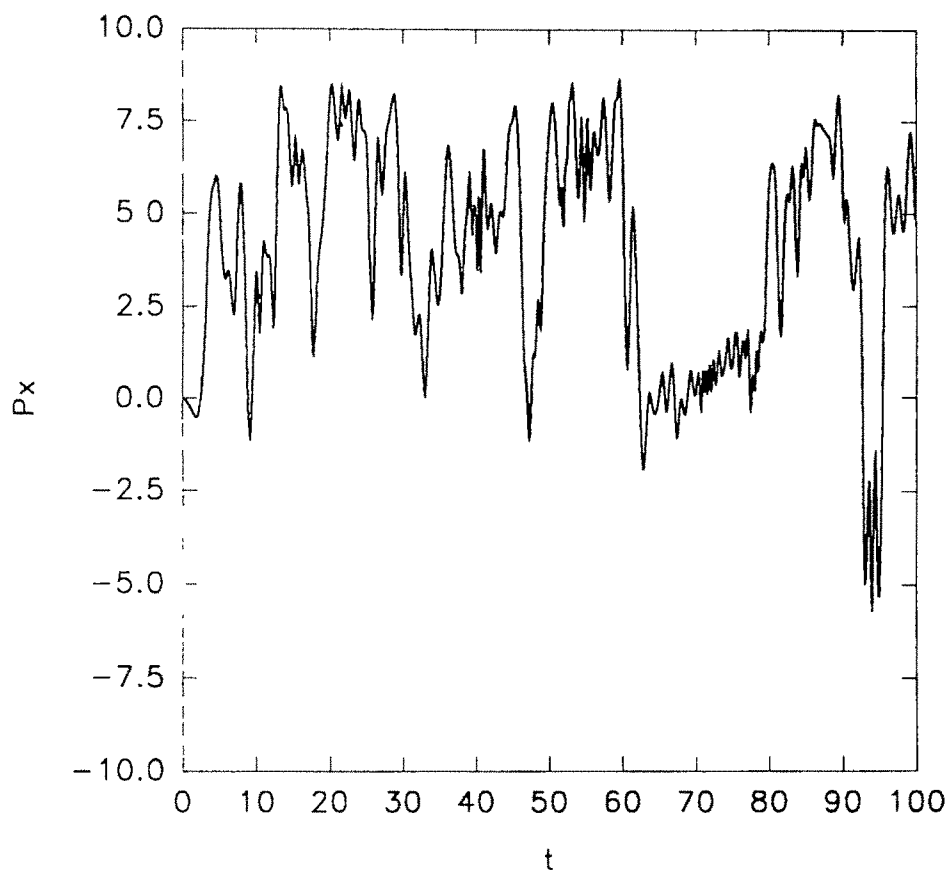


Fig 2b

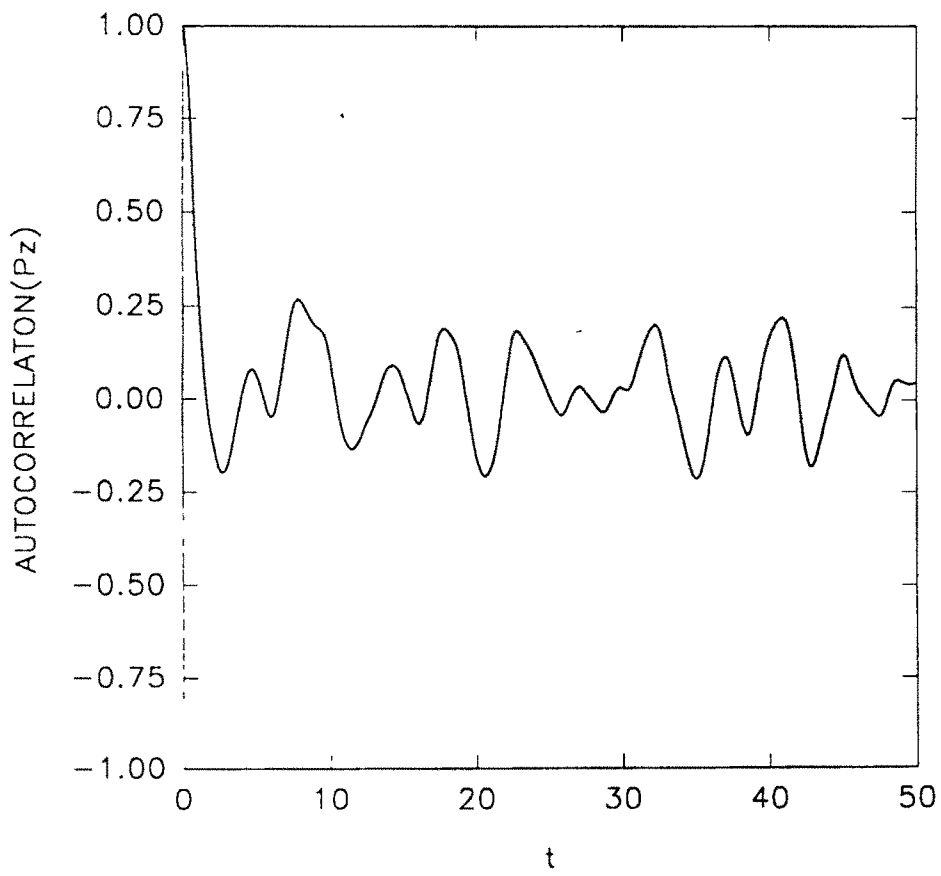


Fig 2c

This is an abelian case

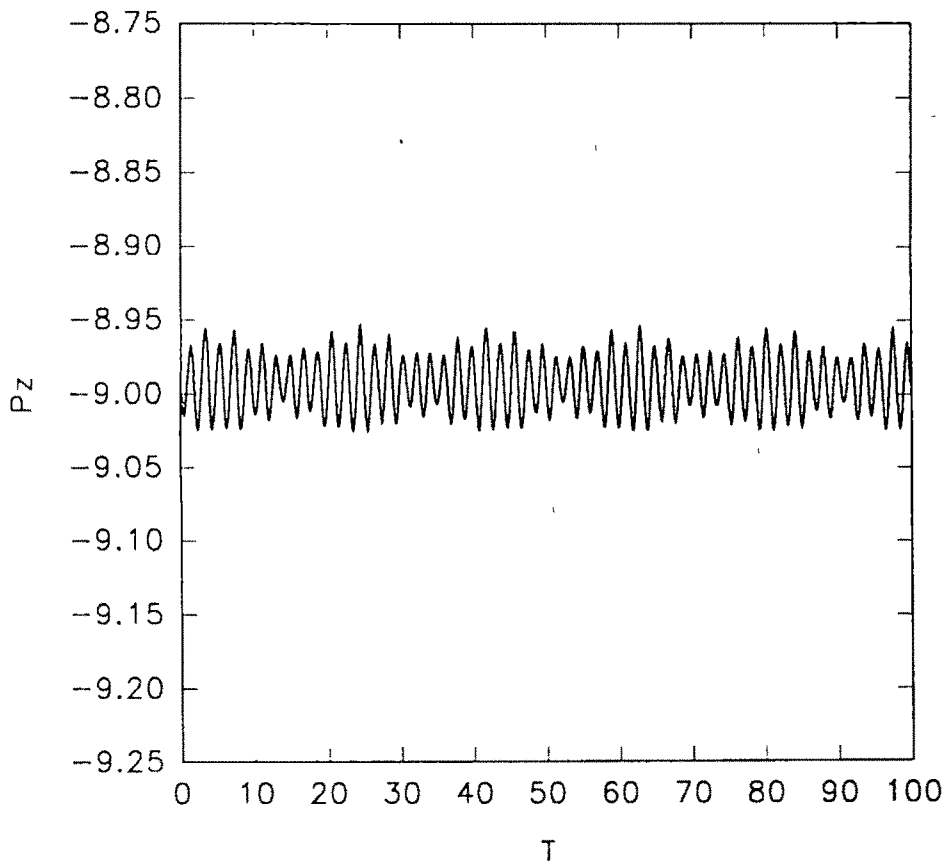


Fig 3